STM JOURNALS

Journal of
Polymer & Composites

ISSN: 2321-2810 (Online)
ISSN: 2321-8525 (Print)
Volume 11, Special Issue 8, 2023
DOI (Journal): 10.37591/JoPC

http://engineeringjournals.stmjournals.in/index.php/JoPC/index

Research JoPC

Fracture Behavior of 2124Al-10vol% SiCp Composite Tensile Specimens for Different Heat Treatment Conditions

T. Parameshwaran Pillai[1], K.S. Sajikumar[2], K. Prasanth Kumar Reddy[3,*], Boggarapu Nageswara Rao[4]

Abstract

This article presents experimental details on 2124Al-10vol% SiCp composite tensile specimens, which were made by squeeze casting process. Cast metal composites are generally very brittle and have poor mechanical properties. To strengthen the matrix and improve ductility, the specimens were heat-treated by solutionizing and aging. Experiments were carried out at 3 different solutionizing temperatures, solutionizing time, aging temperature and aging time to examine the influence of heat treatment process parameters on the notched and unnotched tensile strength of the composite. Compact tension (CT) specimens with different crack lengths, crack mouth widths and thicknesses were tested to evaluate the fracture toughness of the composite. Experiments were planned according to the Taguchi's L9 OA (orthogonal array). Factographs of tensile and CT specimens were made after the test using a scanning electron microscope (SEM). Energy dispersive X-ray analysis was carried out at different locations of the fractured specimens. The EDAX spectrum shows the chemical composition of inclusions and matrix components.

Keywords: EDAM spectrum; Fracture toughness; Metal matrix composites; SEM; Taguchi method; Tensile strength.

***Author for Correspondence**
Prasanth Kumar Reddy

[1]Assistant Professor, Department of Mechanical Engineering, University College of Engineering, BIT Campus, Tiruchirappalli, Tamil Nadu, India
[2]Associate Professor, Department of Mechanical Engineering, Koneru Lakshmaiah Education Foundation (KLEF), Deemed to be University, Green Fields, Vaddeswaram, Guntur, Andhra Pradesh, India
[3]Research Scholar, Department of Mechanical Engineering, College of Engineering Trivandrum, Thiruvananthapuram, Kerala India
[4]Professor, Department of Mechanical Engineering, College of Engineering Trivandrum, Thiruvananthapuram, Kerala India

Received Date: November 28, 2023
Accepted Date: December 23, 2023
Published Date: February 01, 2024

Citation: T. Parameshwaran Pillai, K.S. Sajikumar, K. Prasanth Kumar Reddy, Boggarapu Nageswara Rao. Fracture Behavior of 2124Al-10vol% SiCp Composite Tensile Specimens for Different Heat Treatment Conditions. Journal of Polymer & Composites. 2023; 11(Special Issue 8): S279-S291.

INTRODUCTION

Silicon carbide (SiCp) reinforced aluminum matrix composites have high strength, high specific modulus, high wear resistance, and excellent corrosion resistance, which have broad application prospects in automotive, machinery, aviation, and electronic packaging fields [1, 2]. Addition of SiC particles to aluminum composites improves hardness, density, and compressive strength [3–6]. The mechanical properties of SiC particle-reinforced metal matrix composites (MMCs) are influenced by microstructure and interfacial reactions [7]. The production techniques of centrifugal casting, powder metallurgy, and stir casting offer effective ways to produce aluminum SiC particle MMCs with enhanced properties [8–11]. Aluminum SiC particle MMCs have potential applications in the aerospace industry due to their high strength, lightweight design, wear resistance, and corrosion resistance [12–14].

Al-SiC 2124 composites are usually made by the powder metallurgy route, avoiding the use of liquid metal, which would create a brittle reaction zone of Al4C3 around the reinforcement. Prasad and Sasidhara [15] have compiled flow stress data for 2124 aluminum with varying volume fractions of SiC particulate (15 μm) reinforcements in the vacuum hot pressed and extruded at 500˚C for 30 minutes. The nominal composition of the matrix (2124Al) in wt% was 4.2 Cu, 0.99 Mg, 0.72Mn, 0.16Fe, 0.13 Si, 0.03Zn, balance aluminum. 2124AA with 10vol% SiCp exhibits large, grained matrix structure, which restricts the occurrence of super plasticity due to dynamic recrystallization. The material exhibits flow instability in the temperature range 340-420˚C and at strain rates higher than 1s-1. 2124 Al-30vol%SiCp metal matrix composite is difficult to process due to its high SiCp content. Murty et al. [16] investigated the hot working characteristics of 2124Al-SiCp metal matrix composites. The mechanical properties of AlMMCs generally lie somewhere between those of unreinforced aluminum and titanium alloys. However, it is possible to alter the balance of properties by careful selection of matrix alloy and level of reinforcement.

Inspired by the work of previous researchers, this paper investigates the fracture behavior of 2124Al-10vol% SiCp composite tensile specimens for different heat treatment conditions. To strengthen the matrix and improve ductility, the specimens were heat-treated by solutionizing and aging. Experiments were conducted to verify the influence of heat treatment process parameters on the notched and unnotched tensile strength of the composites and presented the SEM factographs of the tested samples. Energy dispersive X-ray analysis was performed on fractured specimens. The EDAX spectrum shows the chemical composition of inclusions and matrix components.

SPECIMEN TESTING OF 2124Al-10vol% SiCp COMPOSITES

Compact tension (CT) specimens (see Figure 1) with different crack lengths, crack mouth widths and thicknesses were tested to evaluate the fracture toughness of the composite. Tests were planned according to the Taguchi's L_9 OA (orthogonal array). Tensile strength and fracture toughness properties of the 2124Al-10vol% SiCp composite were generated for different heat-treatment conditions. The samples were heat-treated by solutionizing and aging using an Indfur electric furnace. Tensile specimens were tested on a 50T capacity UTM. Fracture toughness testing was performed on an Instron Servo hydraulic controlled dynamic testing machine (8801 model).

Nine blanks of 50 × 50 × 7.5 mm, 50 × 50 × 10 mm, 50 × 50 × 12 mm were cut from the extrusion and machined to final dimensions of CT specimens as per ASTM E399 standards. Specimens were notched to L-T orientation. Special care was taken when pre-cracking the specimens with fatigue cracks of controlled lengths. Because early attempts to produce pre-crack by conventional methods using cyclic tensile loading failed due to the rapid propagation of fatigue cracks. To control this pre-cracking problem, fatigue loading with both minimum and maximum loads in compression was used first to initiate pre-cracks. After that, the initial pre-cracking will stop by self-arrest. Afterwards, the pre-crack can be safely extended to the desired length by additional fatigue loading in tension. Following the above procedure, the specimens were successfully pre-cracked in compression with cyclic loadings of 920 and 5.4 kgf. When the crack self-arrested, the loads were changed to 261 and 27.6 kgf in tension to complete the pre-cracking process. In all cases, the cyclic frequency was 6 Hz.

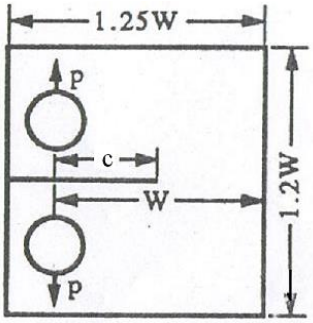

Figure 1. Compact Tension (CT) Specimen.

RESULTS AND DISCUSSION

In the plan of experiments, four factors (viz., solutionizing temperature, solutionizing time, aging temperature and aging time) were selected at three levels. Table 1 gives the factors and the assignment of the corresponding level for which the values taken by the factors. Before selecting an OA (orthogonal array), the minimum number of experiments to be conducted shall be fixed, which is given by [17]

$N_{Taguchi}$ = 1 + Number of factors x (number of levels – 1)= 1 + 4 x (3-1) = 9.

The OA chosen was the L_9 (3^4). The plane of experiments in Table 2 is made of 9 tests (array rows) where the first column was assigned to solutionizing temperature, the second to the solutionizing time, third to aging temperature and fourth to aging time.

The stress intensity factor (K_I) for Compact Tension (CT) specimen is [18]

$$K_I = \frac{P}{B\sqrt{i_*}}\ Y\left(\frac{c}{W}\right), \tag{1}$$

where $Y(\xi) = (2+\xi)(1-\xi)^{-\frac{3}{2}}(0.886 + 4.64\xi - 13.32\xi^2 + 14.72\xi^3 - 5.6\xi^4)$. P is the load; B is the thickness; W is the width and c is crack length of the CT specimen. Using ANSYS, finite element analysis (FEA) has been carried out to evaluate $\boldsymbol{K_I}$ of the CT specimen. Half the model (see Figure 2) is considered and applied the symmetry boundary conditions. FEA results are found to be in good agreement with the expression (1) for $\boldsymbol{K_I}$.

The elastic nominal (net section) stress at failure, σ_{nf}, for CT specimen is [19–22]:

$$\sigma_{nf} = \frac{2P_{max}}{BW}\left(2 + \frac{c}{W}\right)\left(1 - \frac{c}{W}\right)^{-2} \tag{2}$$

where $P_{max}$is the failure load. The fracture toughness (K_Q) is obtained by substituting the failure load, P_{max} for P in equation (1).

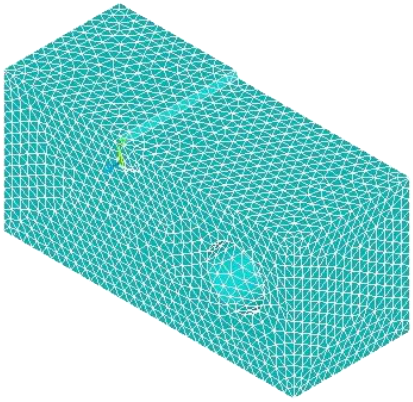

Figure 2. Half the FE model of CT specimen.

Table 1. Assignment of the levels to the factors.

Level	Factors			
	Solutionizing		***Aging***	
	Temperature (°C)	*Time (hrs)*	*Temperature (°C)*	*Time (hrs)*
1	500	6	180	10
2	520	8	200	12
3	540	10	220	14

Table 2 gives tensile strength (σ_0), failure load (P_{max}) of CT specimens, and fracture toughness (K_Q) of the composite. Using the measured output responses from Table 2, analysis of variance (ANOVA) is performed and presented the results in Table 3. Solutionized temperature (S_T) has maximum influence on σ_0 with 80 % Contribution, while 65 %Contribution on K_Q. The influence of other parameters (St, A_T and A_t) on σ_0 are: 12.5%, 2 % and 5.5 % respectively. The influence of parameters (St, A_T and A_t) on K_Q are: 17.4 %, 2.7 % and 15.4 % respectively. The grand mean value of σ_0= 265.4 MPa and the grand mean value of K_Q= 18.06 $MPa\sqrt{m}$. Figure 3 shows the fractured CT specimen.

From the mean values of the output responses ($\sigma_0$and K_Q) in ANOVA Table 3, it is possible to estimate the output responses for the specified levels of the process parameters using the additive law [17]:

$$\hat{\varphi} = \sum_{i=1}^{n_p} \bar{\varphi}_{ik} - (n_p - 1)\varphi_g \quad (3)$$

Here, $\hat{\varphi}$ is the estimate of the output response. $\varphi_g$is the grand mean of the output response. $\bar{\varphi}_{ik}$is the mean value of the output response corresponding to i[th] process parameter (i.e., i = 1 for S_T; i = 2 for S_t; i = 3 for A_T; and i = 4 for A_t) and k[th] level (i.e., k = 1,2,3). Estimates of $\sigma_0$and K_Q using equation (3) are exactly matching with the measured data in Table 2.

Table 2. Taguchi's L_9 OA and values of tensile strength (σ_0), failure load (P_{max}) and fracture toughness (K_Q) of CT specimen (Width (W) = 32 mm; Thickness (B) = 7.5 mm; Initial crack size (c) = 10 mm).

Test runs	Solutionizing		Aging		Tensile strength, σ_0 (MPa)	Failure load, P_{max} (kN)	Fracture toughness, K_Q ($MPa\sqrt{m}$)
	Temp., S_T (°C)	*Time, S_t (hrs)*	*Temp., A_T (°C)*	*Time, A_t (hrs)*			
1	500	6	180	10	277	4.294	18.58
2	500	8	200	12	335	3.338	14.44
3	500	10	220	14	300	3.169	13.71
4	520	6	200	14	177	3.784	16.37
5	520	8	220	10	222	4.065	17.59
6	520	10	180	12	209	3.812	16.49
7	540	6	220	12	298	5.800	25.10
8	540	8	180	14	314	4.309	18.65
9	540	10	200	10	257	5.001	21.64

Table 3. ANOVA results on performance characteristics (σ_0 and K_Q)

Parameters	1st Mean	2nd Mean	3rd Mean	SoS	%Contribution
Tensile strength, σ_0 : Grand mean = 265.4 MPa					
S_T (°C)	304.0	202.7	289.7	18043	80.0
S_t (hrs)	250.7	290.3	255.3	2820	12.5
A_T (°C)	266.7	256.3	273.3	440	2.0
A_t (hrs)	252.0	280.7	263.7	1247	5.5
Fracture toughness, K_Q : Grand mean = 18.06 MPa $\sqrt{m}$					
S_T (°C)	15.577	16.817	21.797	65.0	65.0
S_t (hrs)	20.017	16.893	17.280	17.4	17.4
A_T (°C)	17.907	17.483	18.800	2.7	2.7
A_t (hrs)	19.270	18.677	16.243	15.4	15.4

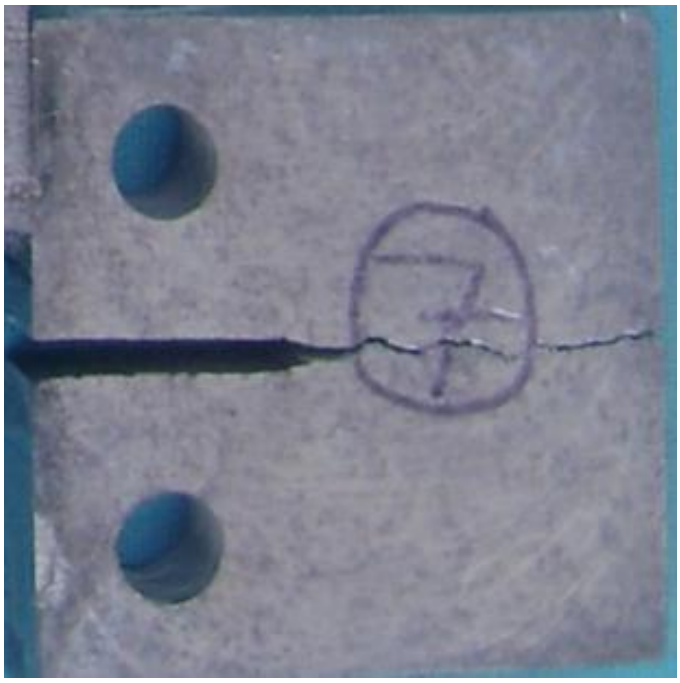

Figure 3. Fractured CT specimen.

Considering the mean values of $\sigma_0$and K_Q from ANOVA Table 3 and the additive law in equation (3), empirical relationships are developed in terms of S_T, St, A_T and A_t in the form:

$$\sigma_0 = 233.67 - 7.1667\xi_1 + 94.1667\xi_1^2 + 2.3333\xi_2 - 37.3333\xi_2^2 + 3.3333\xi_3 + 13.6667\xi_3^2 + 5.8333\xi_4 - 22.8333\xi_4^2 \quad (4)$$

$$K_Q = 15.68 + 3.11\xi_1 + 1.87\xi_1^2 - 1.3683\xi_2 + 1.7555\xi_2^2 + 0.4467\xi_3 + 0.87\xi_3^2 - 1.5133\xi_4 - 0.92\xi_4^2 \quad (5)$$

Here, $\xi_1 = 0.05S_T - 26$; $\xi_2 = 0.5S_t - 4$; $\xi_3 = 0.05A_T - 10$; and $\xi_4 = 0.5A_t - 6$.

From the mean values of the output responses in ANOVA Table-3, maximum σ_0 mean values correspond to the 1st level of S_T, 2nd level of S_t, 3rd level of A_T and 2nd level of A_t. Hence, σ_{0max} (maximum σ_0) can be achieved for a set of parameters ($S_{T1}S_{t2}A_{T3}A_{t2}$). Number subscripts indicate the level of the parameters. Similarly, a set of parameters ($S_{T3}S_{t1}A_{T3}A_{t1}$) was found for maximum K_Q ($K_{Q\,max}$). Two different sets of parameters found for σ_{0max} and K_{Qmax}. The designer needs a set of parameters to achieve simultaneously σ_{0max} and $K_{Q\,max}$. Hence, multi-objective optimization scheme [23–26] is appropriate to have a set of parameters for achieving σ_{0max} and $K_{Q\,max}$. These objectives have different units of measurement. To handle such problems, all the output responses are normalized and converted to maximization of a single objective function [25]:

$$\zeta = \omega_1\zeta_1 + \omega_2\zeta_2 \quad (6)$$

Here, $\zeta_1 = \frac{\sigma_0}{\sigma_{0max}}$; $\zeta_2 = \frac{K_Q}{K_{Qmax}}$; $\omega_1$and $\omega_2$are the positive weighing factors such that $\omega_1 + \omega_2 = 1$; σ_{0max} = 352 MPa; and $K_{Q\,max}$ = 25.69 $MPa\sqrt{m}$. Maximizing ζ, results in high $\sigma_0$and high K_Q. Assuming $\omega_1 = \omega_2 = 0.5$, and using mean values of σ_0 and K_Q from ANOVA Table 3 in equation (6), ANOVA results for ζ are obtained (see Table 4). A set of parameters ($S_{T3}S_{t1}A_{T3}A_{t2}$) found from the maximum mean values of ζ. Hence, optimal parameters to attain maximum ζ are: S_T = 540°C; S_t = 6 hours; A_T = 220°C; and A_t = 12 hours. The output responses corresponding to the set of optimal parameters obtained from equations (4) and (5) are: σ_0= 297.84 MPa and K_Q = 25.1 $MPa\sqrt{m}$ (see Table 5), which are matching well with the measured data.

Table 4. ANOVA for ζ

Parameters	1st Mean	2nd Mean	3rd Mean
S_T (°C)	0.7350	0.6152	0.8357
S_t (hrs)	0.7456	0.7412	0.6990
A_T (°C)	0.7273	0.7044	0.7542
A_t (hrs)	0.7330	0.7622	0.6907

Table 5. Estimates of strength (σ_0) and fracture toughness (K_Q)

Solutionizing		Aging		Strength	Fracture toughness
Temp., S_T (°C)	***Time, S_t (hrs)***	***Temp., A_T (°C)***	***Time, A_t (hrs)***	***σ_0 (MPa)***	***K_Q ($MPa\sqrt{m}$)***
Case study-I: Single-objective optimization Set of optimal parameters ($S_{T1}S_{t2}A_{T3}A_{t2}$) for maximum σ_0					
500	8	220	12	351.84	15.76
Case study-II: Single-objective optimization Set of optimal parameters ($S_{T3}S_{t1}A_{T3}A_{t1}$) for maximum K_Q					
540	6	220	10	269.17	25.69
Case study-III: Multi-objective optimization Set of optimal parameters ($S_{T3}S_{t1}A_{T3}A_{t2}$) for maximum $\sigma_0$and maximum K_Q					
540	6	220	12	297.84 (298)+	25.1 (25.1)
+ Measured data					

Table 6. Effect of thickness (B) on the fracture toughness of the CT specimens for S_T = 500°C; S_t = 12 hours; A_T = 200°C; and A_t = 12 hours. (Width, W = 32 mm; Tensile strength, σ_0 = 282 MPa)

Crack Length, c (mm)	Thickness, B (mm)	Crack Mouth Width (mm)	Failure load, P_{max} (kN)	Net section Stress, σ_{nf} (MPa)	Fracture toughness, K_Q ($MPa\sqrt{m}$)
10	7.5	1.2	4.953	201.9	21.43
13.33	10	1.4	5.030	223.2	21.39
16	12	1.6	4.990	259.9	22.45
11	7.5	1.4	4.956	224.8	23.24
14.66	10	1.6	4.325	226.3	20.63
17.6	12	1.2	4.580	300.4	24.25
12	7.5	1.6	4.241	214.9	21.55
16	10	1.2	3.946	246.6	21.31
19.2	12	1.4	3.697	312.9	23.52

Tensile strength (σ_0) of the un-heat-treated composite is 163 MPa, while it is 282 MPa for the heat-treatment process: S_T = 500°C; S_t = 12 hours; A_T = 200°C; and A_t = 12 hours. The effect of thickness on the fracture toughness (K_Q) of the CT specimens is shown in Table 6. It is evidenced from FEA results that the crack mouth width has no effect on K_I. P_{max} decreases with increasing crack size and the average K_Q = 22.2 $MPa\sqrt{m}$.

CT specimens were subjected to hot pressing. Table 7 gives $\boldsymbol{K_Q}$ values for different parameters (viz., temperature and % of compression). The dimensions of the specimens are: Width (W) = 32 mm; Thickness (B) = 7.5 mm; Crack mouth width = 1.2 mm; and Initial crack size (c) = 10 mm. The maximum K_Q = 24.35 $\boldsymbol{MPa\sqrt{m}}$ for the hot-pressing parameters: Temperature = 500°C and 50% of compression.

Table 7. Effect of hot pressing on the fracture toughness (K_Q) of the CT specimens.

Hot pressing parameters		Failure load, P_{max} (kN)	Net section Stress, σ_{nf} (MPa)	Fracture toughness, $K_Q\,(MPa\sqrt{m})$
Temperature (°C)	*% of compression*			
450	15	2.547	103.8	11.02
450	25	4.920	200.6	21.29
500	25	4.726	192.9	20.45
500	50	5.628	229.5	24.35
550	15	5.236	213.5	22.66
550	25	3.717	151.5	16.08
550	50	5.194	211.8	22.47

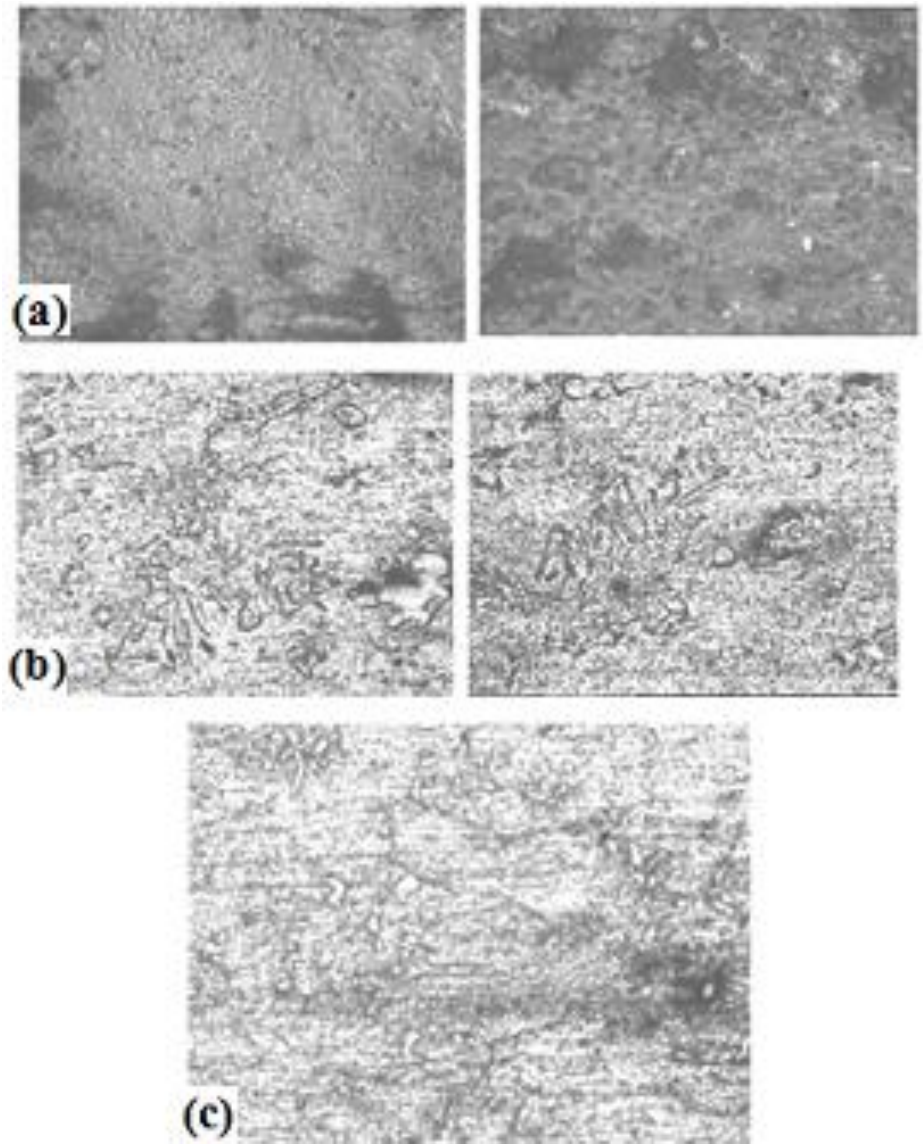

Figure 4. Optical microstructures at different heat-treatment processes: (a) un-heat-treated; (b) S_T = 500°C; S_t = 8 Hrs; A_T = 200°C; A_t = 12 Hrs; and (c) S_T = 540°C; S_t = 8 Hrs; A_T = 180°C; A_t = 14 Hrs.

Fracture in engineering alloys can occur via transgranular (across grains) or intergranular (along grain boundaries) fracture paths. However, regardless of the fracture path, there are 4 principal fracture modes (dimple rupture, cleavage, fatigue and decohesive rupture). Each of these modes has a

characteristic fracture surface and a mechanism or mechanisms by which the fracture propagates. To analyze the fracture surface of the specimens to assess the material quality, fractographs of tested specimens were performed using scanning electron microscope (SEM). Energy dispersive X-ray analysis was carried out at different locations of the fractured specimens. EDAX spectrums show chemical composition of inclusions and matrix components. Figure 4 shows the optical microstructures at different heat-treatment processes. SEM of tensile specimens at heat-treatment process (S_T = 500°C; S_t = 8 Hrs; A_T = 200°C; A_t = 12 Hrs) in Figure 5(a) shows combined intergranular decohesion and trans granular cleavage like fracture, while Figure 5(b) for the heat-treatment process (S_T = 540°C; S_t = 8 Hrs; A_T = 180°C; A_t = 14 Hrs) shows transition from intergranular mode to dimple mode of failure, and blight inclusion of SiC (Stringer type) by cleavage. SEM and EDAX spectrum of CT specimens in Figure 6 at S_T = 500°C; S_t = 8 Hrs; A_T = 200°C; A_t = 12 Hrs depicting the failure along intergranular facets (see different sizes of SiC particles).

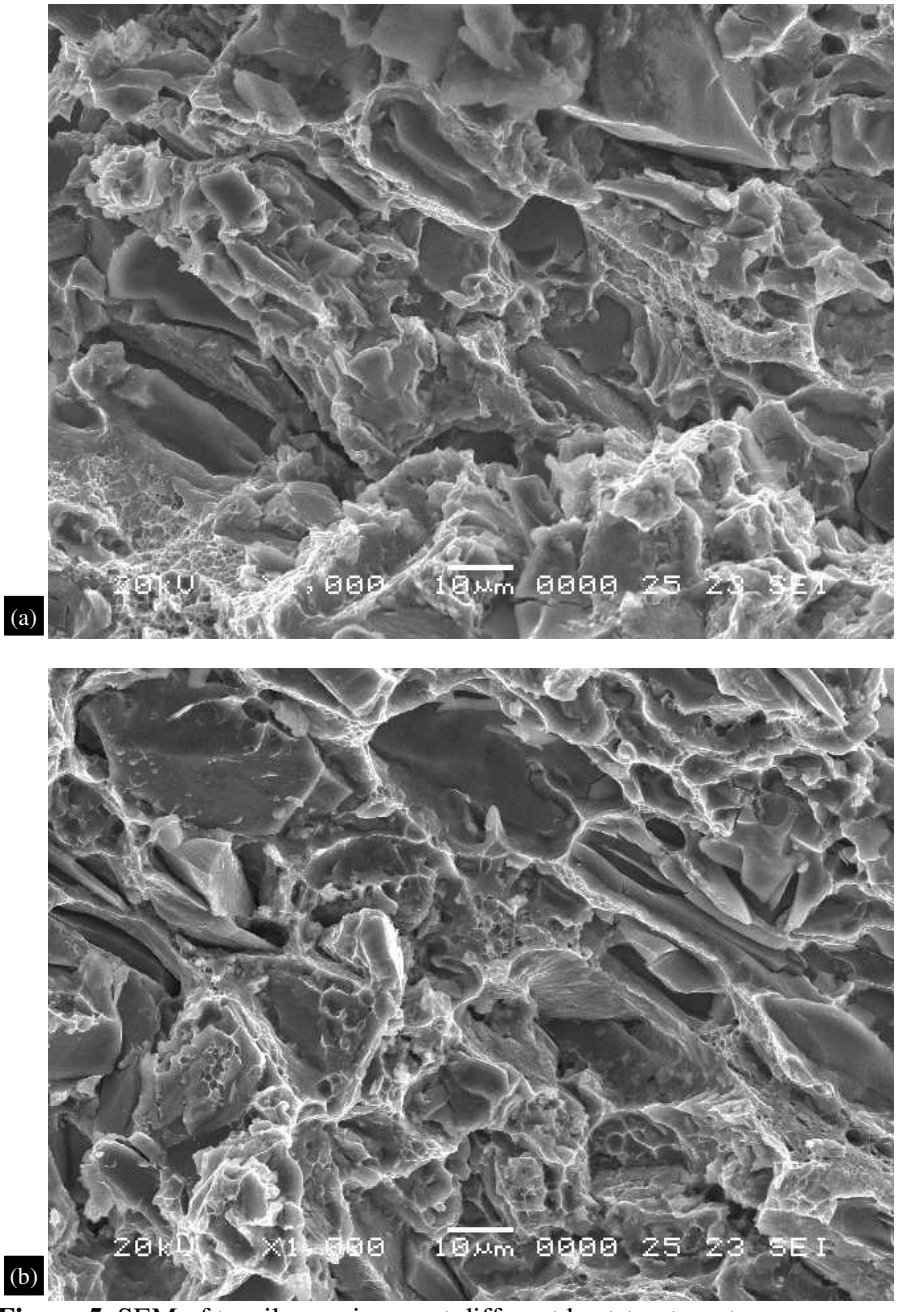

Figure 5. SEM of tensile specimens at different heat-treatment processes.

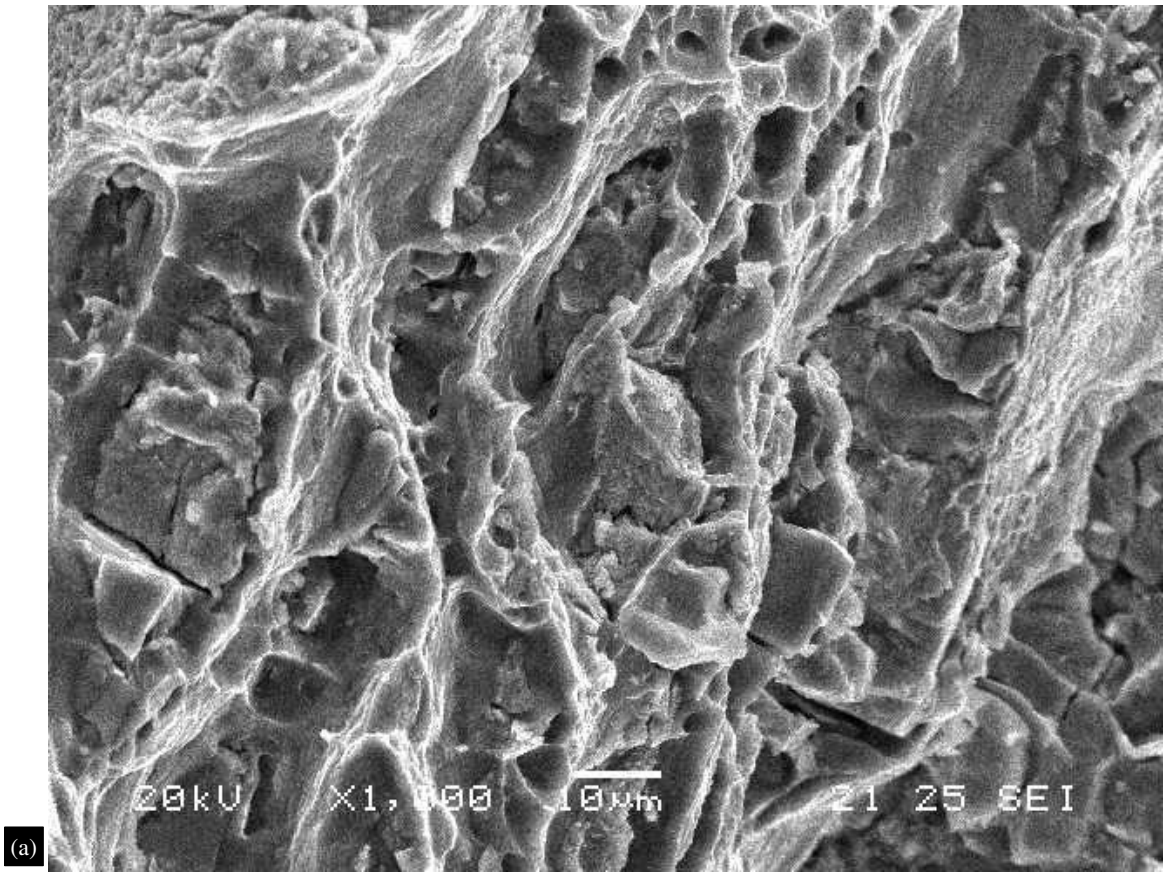

(a)

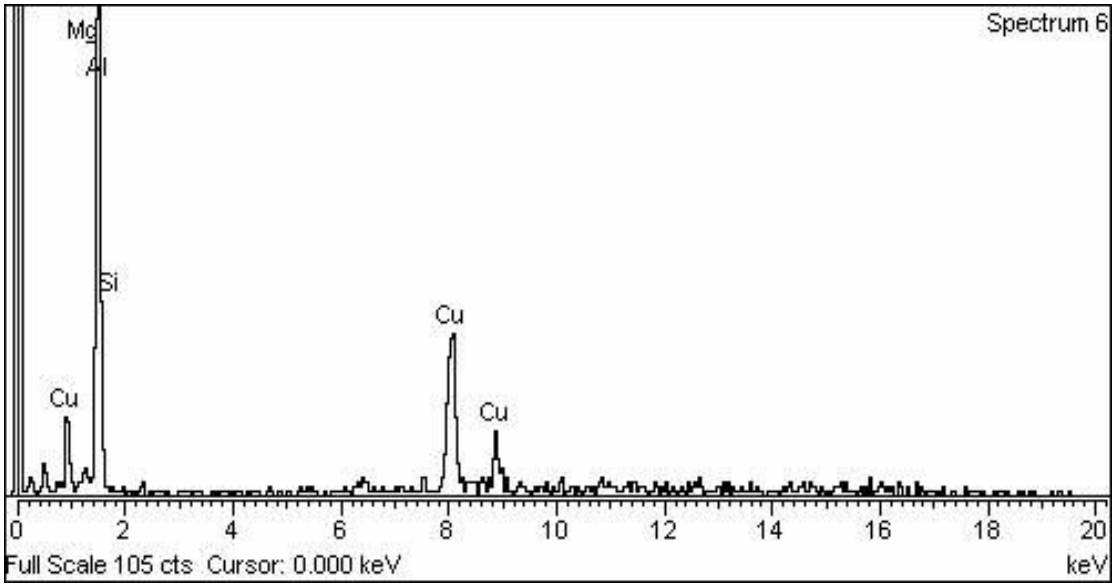

(b)

Figure 6. SEM and EDAX spectrum of CT specimen at heat-treatment-process: S_T = 500°C; S_t = 8 Hrs; A_T = 200°C; A_t = 12 Hrs.

SEM and EDAX spectrum of CT specimen for the heat-treatment-process (S_T = 540°C; S_t = 8 Hrs; A_T = 180°C; A_t = 14 Hrs) in Figure 7 shows large number of dimples along with intergranular voids (mixed mode of failure). Figure 8 shows the scanning electron micrographs and EDAX spectrum of CT specimens for the hot-pressing parameters: Temperature = 450°C; % of compression = 15, whereas Figure 9 shows for the hot-pressing parameters: Temperature = 500°C; % of compression = 50.

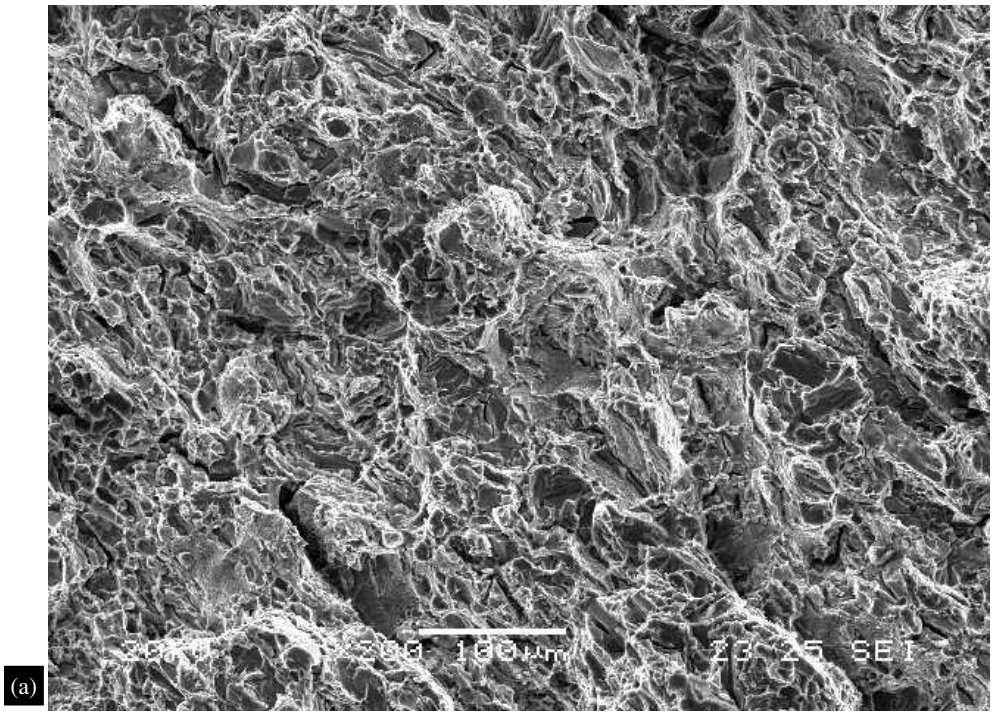

Figure 7. SEM and EDAX spectrum of CT specimen for the heat-treatment-process (S_T = 540°C; S_t = 8 Hrs; A_T = 180°C; A_t = 14 Hrs).

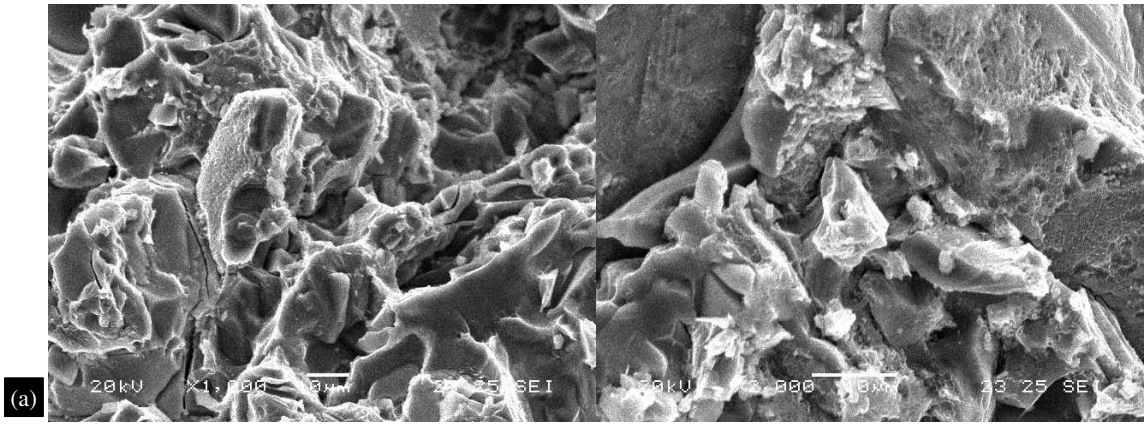

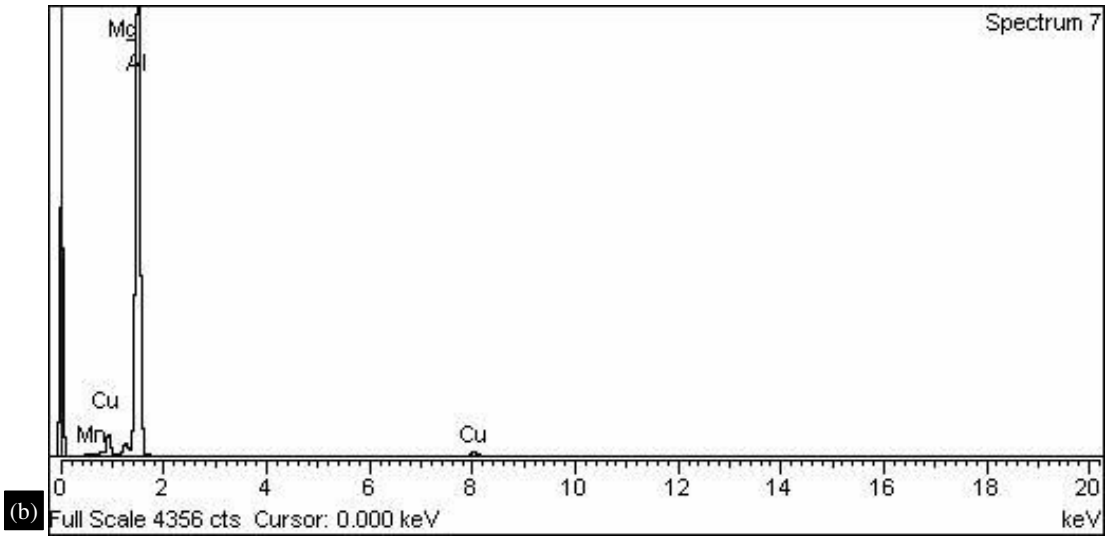

Figure 8. SEM and EDAX spectrum of CT specimens (Hot pressing parameters:

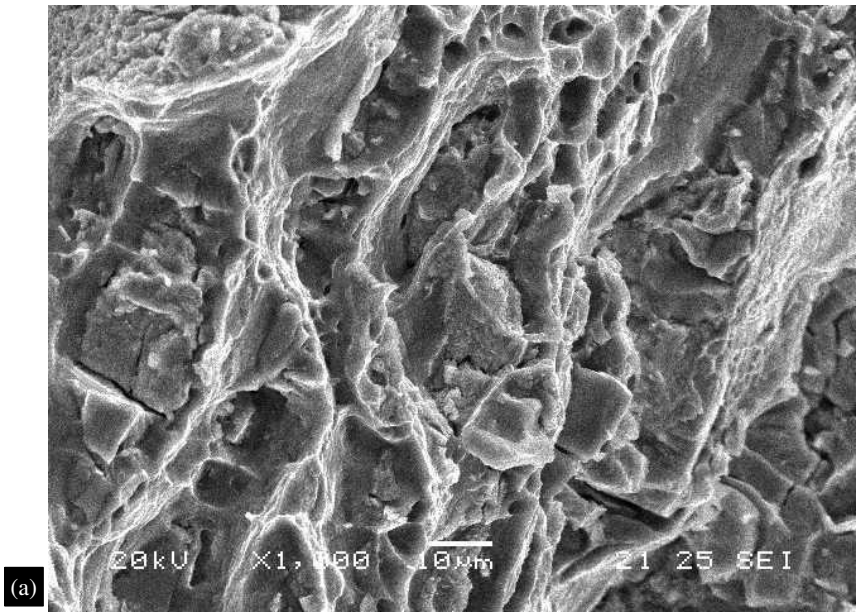

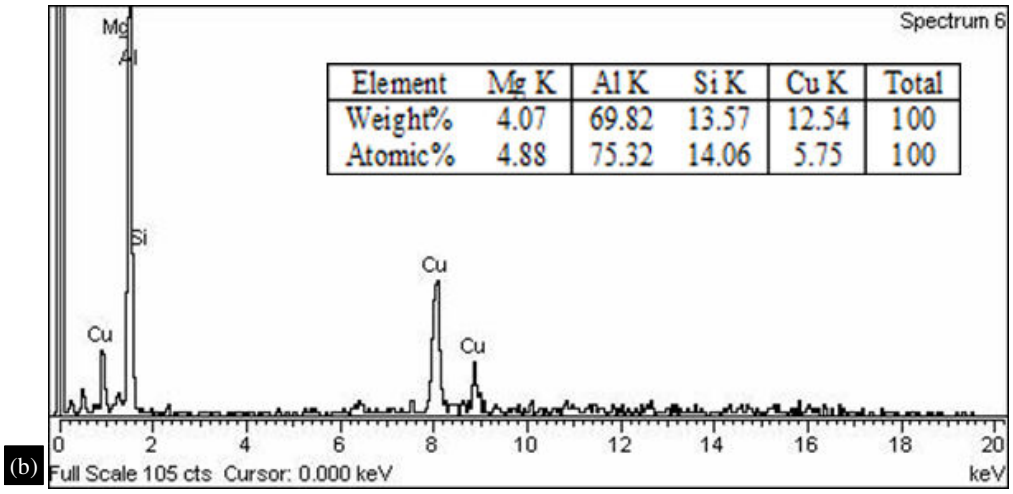

Figure 9. Scanning electron micrographs and EDAX spectrum of CT specimens. (Hot pressing parameters: Temperature = 500°C; % of compression = 50).

CONCLUSIONS

This paper deals with the fracture behavior of 2124Al-10vol% SiCp composite tensile specimens under different heat treatment processes. Taguchi's L_9 OA (orthogonal array) is selected for the 4 process variables with 3 levels of each variable. The 4 process variables are solutionizing temperature (S_T), solutionizing time (S_t), aging temperature (A_T) and aging time (A_t), the effect of which is evaluated on the notched and un-notched tensile strength of the composite. Fracture toughness (K_Q) of composites is evaluated by conducting tests on Compact tension (CT) specimens. Scanning electron microscope (SEM) is used to generate factographs on tested tensile and CT specimens. Energy dispersive X-ray analysis was carried out at different locations of the fractured specimens. The chemical composition of the inclusions and matrix components was characterized in EDAX spectrums.

REFERENCES

1. Y. Wang, L. Ren, F. Yang, L. Qi, C. Yu, H. Luo, "Research Progress on Fabrication Technology and Properties of SiC Particle-Reinforced Aluminum Matrix Composites", *Xiyou Jinshu Cailiao Yu Gongcheng/Rare Metal Materials and Engineering,* Vol. 51, Issue 4, pp.1270–1282 (2022)
2. S. Thirugnanam, G. Ananth, T. Muthu Krishnan, T.T. Olkeba, "Microstructure and Mechanical Characteristics of Stir-Casted AA6351 Alloy and Reinforced with Nanosilicon Carbide Particles", Journal of Nanomaterials, Vol. 2023, Article ID 7858827. https://doi.org/10.1155/2023/7858827
3. P.P. Shantharaman, V. Anandakrishnan, S. Sathish, M. Ravichandran, R. Naveenkumar, S. Jayasathyakawin, S. Rajesh, "Investigations on the microstructure and properties of yttria and silicon carbide reinforced aluminium composites", Heliyon, 9(4) April 2023, e15462. https://doi.org/10.1016/j.heliyon.2023.e15462
4. Y. Xing, N.Y. Li, C.J. Li, P. Gao, H.D. Guan, C.M.Y. Yang, C.J. Pu [a], J.H. Yi, "Effects of size and oxidation treatment for SiC particles on the microstructures and mechanical properties of SiCp/Al composites prepared by powder metallurgy", Materials Science and Engineering: A, Vol. 851 (2022) 143664. https://doi.org/10.1016/j.msea.2022.143664
5. M. Hamza, S. Mondal, "Effect of Reinforcement with Ceramic Microparticles on Structure and Properties of Composites with an Aluminum Matrix", *Met Sci Heat Treat* 64, 163–166 (2022). https://doi.org/10.1007/s11041-022-00778-x
6. M. Khodaei, O. Yaghobizadeh, H.R. Baharvandi, A.A. Shahraki, H. mohammadi, "The effect of nano-TiO_2 additions on the densification and mechanical properties of SiC-matrix composite", Ceramics International, Vol.46, Issue 5, pp. 6477-6483 (2020).
7. Y. Wang, T. Monetta, "Systematic study of preparation technology, microstructure characteristics and mechanical behaviors for SiC particle-reinforced metal matrix composites", Journal of Materials Research and Technology, Vol.25, pp.7470-7497 (2023). https://doi.org/10.1016/j.jmrt.2023.07.145
8. M. Łągiewka, C. Kolmasiak, "Composite centrifugal castings after remelting", Metalurgija, Vol.60, No.3-4 (2021). https://hrcak.srce.hr/256131
9. A.K.B. Chellam, M. Pandian, D. Jaganathan, M.S.R. Mydeen, K. Kalimuthu, "Analysing the mechanical and metallurgical behavior of aluminium 7075 composite with reinforcement of silicon carbide and zirconium oxide", *AIP Conf. Proc.* 2527, 020019 (2022). https://doi.org/10.1063/5.0108139
10. K.S.K. Reddy, M. Kannan, R. Karthikeyan, *et al.* "Evaluation of mechanical and thermal properties of Al 7475–CSA–graphite hybrid metal matrix composites", *Int J Interact Des Manuf* (2023). https://doi.org/10.1007/s12008-023-01401-w
11. R.K. Bhushan, D. Sharma, "Optimization of Friction Stir Welding Parameters to Maximize Hardness of AA6082/Si_3N_4 and AA6082/SiC Composites Joints", *Silicon* 14, 643–661 (2022). https://doi.org/10.1007/s12633-020-00894-4
12. Y. Wang, T. Monetta, "Systematic study of preparation technology, microstructure characteristics and mechanical behaviors for SiC particle-reinforced metal matrix composites", Journal of Materials Research and Technology, Vol. 25, pp. 7470-7497 (2023). https://doi.org/10.1016/j.jmrt.2023.07.145

13. A. Kumar, R.C. Singh, R. Chaudhary, V.P. Singh, " Tribological studies and Microstructural characterisation of SiC and Fly Ash Particles Based Aluminium 2024 alloy Composites Prepared through Stir Casting Route", 2020 *IOP Conf. Ser.: Mater. Sci. Eng*. 804 012025.DOI 10.1088/1757-899X/804/1/012025
14. A. Schmidt, S. Siebeck, U. Götze, G. Wagner, D. Nestler, "Particle-Reinforced Aluminum Matrix Composites (AMCs)—Selected Results of an Integrated Technology, User, and Market Analysis and Forecast", *Metals* 2018, *8*, 143. https://doi.org/10.3390/met8020143
15. Y.V.R.K. Prasad and S. Sasidhara, "Hot Working Guide- A Compendium of Processing Maps", ASM Metals Park, OH, USA (1997).
16. S.V.S.N. Murty, B. Nageswara Rao and B.P. Kashyap, "On the hot working characteristics of 2124Al-SiCp metal matrix composites", Advanced Composite Materials, Vol.11, pp.105-120 (2002).
17. P.J. Ross, "Taguchi Techniques for Quality Engineering", McGraw- Hill, Singapore (1989).
18. Y. Murakami, "Stress intensity factors hand book" (in two volumes), Pergamon press, New York (1987).
19. J.C. Newman, Jr., "An evaluation of fracture analysis methods", Elastic-Plastic Fracture Mechanics Technology, ASTM-STP-896, pp.5-96 (1985).
20. ASTM E399-83, Standard test method for plane-strain fracture toughness of metallic materials. Annual Book of ASTM standards, Vol.03.01, pp.487-511 (1989).
21. J.E. Srawley, "Wide range stress intensity factor expressions for ASTM E399 standard fracture toughness specimens", Int.J.Fracture, Vol.12, pp.475-476 (1976).
22. R.A. Saxena and S.J. Hundak, "Review and extension of compliance information for common crack growth specimens", Int.J.Fracture, Vol.14, pp.453-486 (1978).
23. B.V. Dharmendra, S.P. Kodali, B. Nageswara Rao, "A simple and reliable Taguchi approach for multi-objective optimization to identify optimal process parameters in nano-powder-mixed electrical discharge machining of INCONEL800 with copper electrode", HELIYON 5, e02326 (2019). https://doi.org/10.1016/j.heliyon.2019.e02326.
24. B.V. Dharmendra, S.P. Kodali, B. Nageswara Rao, "Multi-objective optimization for optimum abrasive water jet machining process parameters of Inconel718 adopting the Taguchi approach", Multidiscip. Model. Mater. Struct. 16:2, 306–321 (2020). https://doi.org/10.1108/MMMS-10-2018-0175
25. A. Muni Tanuja, B. Tanya, B. Nageswara Rao (2023). Multi-objective optimization basing modified Taguchi method to arrive the optimal die design for CGP of AZ31 magnesium alloy, International Journal on Interactive Design and Manufacturing (IJIDeM), Springer Nature. https://doi.org/10.1007/s12008-022-01176-6
26. Reddy, K.P.K., Rao, B.N., Nazeemudheen, M.N. et al. Selection of Optimal Process Parameters to Obtain Defect-Free Builds in IN718 Made by Laser Powder Bed Fusion. J. of Materi Eng and Perform (2023). https://doi.org/10.1007/s11665-023-08677-9

